Study of the Symptoms and Distribution Pattern Detection of Ring Spot Disease (*Leptosphaeria* sp.) on Sugarcane Plants Using Aerial Images

A D Indrawan[1], H Nirwanto[1], W Windriyanti[1], and W W Jati[2]

[1]Master of Agrotechnology Study Program, Faculty of Agriculture, UPN "Veteran" Jawa Tmur, Indonesia
Jl. Rungkut Madya, Gunung Anyar, Kota Surabaya, Jawa Timur, 60249, Indonesia
[2]Indonesian Sugar Research Institute (ISRI)
Jl. Pahlawan No. 25, Panggungrejo, Kota Pasuruan, Jawa Timur, 67126, Indonesia
herry_n@upnjatim.ac.id

Abstract. Productivity of sugarcane (*Saccharum officinarum*) is influenced by various factors, one of which is ring spot disease caused by the fungus *Leptosphaeria sacchari*. Therefore, it is necessary to make efforts to suppress plant damage through Integrated Plant Disease Control so that proper monitoring information is needed. Unmanned Aerial Vehicle (UAV) in recent years has supported increased accuracy and monitoring efficiency through aerial monitoring in agriculture. This study aims to examine the application of UAV in detecting symptoms and distribution patterns of ring spot disease in sugarcane through aerial imagery analysis (aerial monitoring) and compared to conventional monitoring (ground monitoring). This research was conducted in smallholder sugarcane plantations in Sukodono Sub-District, Sidoarjo District, East Java Province, Indonesia from January to March 2023. This research was carried out using a survey method according to disease targets using two types of observations consisting of conventional observation (ground monitoring) and observation using drones (aerial monitoring). Based on the analysis of aerial image data and the results of ground monitoring observations using a geostatistical approach, it was found that aerial imagery has the potential to be used in detecting symptoms and distribution patterns of ring spot disease with an accuracy of 63±68% detection of aerial images using a correlation regression test. The results of aerial image analysis and ground monitoring shows that the distribution of ring spot disease tends to aggregate. Monitoring based on aerial imagery from drones or UAVs technically has advantages including: shorter detection time, easier to do, and being able to reach areas that are not detected by conventional observations.

Keywords: Geostatistics, Sugarcane, Ring spot disease, UAV.

A. Wafa et al. (eds.), *Proceedings of the 8th International Conference of Food, Agriculture and Natural Resources & the 2nd International Conference of Sustainable Industrial Agriculture (IC-FANRes-IC-SIA 2023)*,
Advances in Biological Sciences Research 41,
https://doi.org/10.2991/978-94-6463-451-8_23

1 Introduction

The productivity of sugarcane (*Saccharum officinarum*) is influenced by various factors, one of which is plant diseases, especially ring spot disease [1, 2]. Ring spot disease of sugarcane is caused by *Leptosphaeria sacchari*. The Leptosphaeria fungus infects the leaves of the sugarcane plant causing premature leaf senescence which can interfere with photosynthesis disrupting plant growth [2, 3]. Therefore, efforts are needed to suppress plant damage due to plant diseases through Integrated Plant Disease Control. The first step in Integrated Plant Disease Control is intensive monitoring to monitor the level and pattern of infection as a material for consideration in determining control decisions [4, 5]. Currently, intensive and accurate monitoring efforts require more human resources so large land areas will require high costs [6]. Therefore, a solution is needed for efficient and effective monitoring actions to monitor large land areas. Unmanned Aerial Vehicle (UAV) in recent years has become a tool for remote sensing through efficient aerial monitoring in agriculture [7, 8]. Aerial monitoring can produce aerial images that can be analyzed to determine the condition of plants in a large area that require minimum monitoring time. According to Akram et al., the specific color spectrum indicates the health condition of the plants [9]. This study aims to examine the application of UAV in detecting symptoms of ring spot disease in sugarcane through aerial imagery analysis (aerial monitoring) and compared with conventional monitoring on ground monitoring.

2 Materials and Methods

This research was conducted at two locations including a sugarcane plantation in Sukodono Sub-District, Sidoarjo District, East Java Province as a monitoring location and the Plant Health Laboratory of the Agriculture Faculty, UPN "Veteran" Jawa Timur Indonesia as a location for data analysis and image processing. This research was conducted from January to March 2023.

This research was conducted using a field survey method on sugarcane plantations aged 7-8 months with a land area of 1520 m^2 every two weeks. Research conducted in the field including the acquisition of aerial images using drones (aerial monitoring) and direct observation of plants to determine disease symptoms and intensity (ground monitoring). In addition, tests were carried out in the laboratory to identify the symptoms and causes of ring spot disease. Secondary data related to the weather obtained from the Meteorology, Climatology, and Geophysics Agency of the Republic of Indonesia.

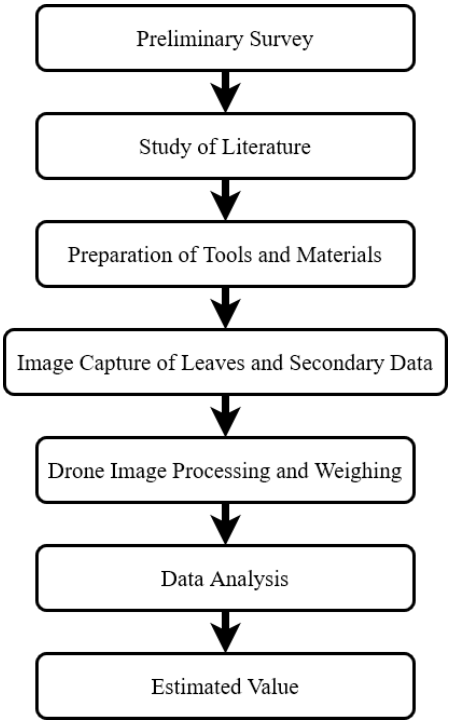

Fig. 1. Research Flowchart

2.1 **Symptoms and Pathogens Identification**

Identification of symptoms of infection was carried out by taking several samples of symptomatic plant leaves and leaves from healthy plants. Symptomatic sugarcane leaves as a result of infection with *Leptosphaeria* sp. are known to have elongated oval spots with pale white spots on the inside and brownish edges on the spots. Healthy plant leaves are light green all over. Wilted leaves of healthy plants are clean yellowish brown without any spots or necrosis due to pests and other diseases. The reference source used in identifying disease symptoms is the Field Guide: Disease of Australian Sugarcane [2]

In vitro test was carried out by isolating symptomatic plant leaves on PDA (Potato Dextrose Agar) media and purification which produced a single colony of the fungus on similar media. Microscopic identification was carried out using an Olympus CX33 microscope with 40x and 100x magnification. Identification of *Leptosphaeria* sp. colony based on the *Mycobiota Associated with Sugarcane (Saccharum officinarum L.) Cultivars in Iraq* [10].

2.2 Aerial Imagery and Data Acquisition

Aerial monitoring includes taking aerial images of the field using the DJI Phantom 4 Pro Drone. Ground Control Point (GCP) as a geospatial reference has been placed at a predetermined point for calibrating the drone's position with the actual location and area measurement. Then the photos were taken at a height of 18 m above the ground to obtain the entire photo of the field.

Ground monitoring or direct observation of plants was carried out in 16 plots measuring 1 m x 1 m. The determination of the sample plots was adjusted based on the purposive sampling method at predetermined points. The specified plants and sample plots are assigned a unique label as a marker. Observations on ground monitoring include observation of symptoms and disease intensity. Retrieval of disease intensity data used the scoring method.

RGB image acquisition was performed using both a UAV (Unmanned Aerial Vehicle) and a smartphone. The UAV captured images using its onboard camera at a height of 20 meters above the ground. The camera on the UAV has a sensor with a capacity of 20 megapixels, allowing it to capture images in the RGB color spectrum, which includes the red, green, and blue channels. For ground monitoring purposes, image capture was also conducted using a Xiaomi Redmi Note 6 Pro smartphone. This involved capturing images of both symptomatic and asymptomatic plant leaves.

2.3 Aerial Image Processing and Analysis

The aerial images were processed and analyzed using a computer equipped with Intel Core i5 10th generation processor and NVIDIA MX330 graphics card. The image processing tasks were performed using Matlab software in the laboratory, including processing, filtering, segmentation, feature extraction, and classification. The aerial images were obtained using a drone based on the specific points in the field, and they are represented in the RGB color space. The RGB color space is a color model that is based on the concept of primary light, namely red, green, and blue [11]. The Matlab software was utilized to extract the R, G, and B values from the images.

Image segmentation is performed to identify specific features within an image and separate them from other elements. The color thresholding technique is utilized in the segmentation process to distinguish the entire plant from the background and to isolate diseased plant parts. Thresholding is conducted in the L^*a^*b color space, which comprises the luminance layer (L^*) and the chromaticity layers (a^* and b^*)[12]. The thresholding operation is executed using the Matlab software with an algorithm that defines a specific range of values [13].

Feature extraction is employed to capture distinguishing characteristics that differentiate one object from another [14]. In this study, color serves as a distinguishing feature for identifying symptomatic sugarcane leaves within the context of the entire sugarcane plant (both healthy and symptomatic). The classification process is carried out to separate healthy plant leaves, symptomatic plant leaves, and other objects. As a result, the outcomes consist of images containing pixels representing the entire plant leaf, as well as images containing pixels representing the symptomatic plant parts.

2.4 Data Analysis

The data acquired from ground monitoring was geostatistically analyzed using variogram and kriging approaches with the SGeMS program [15, 16]. The data obtained from the processing of aerial imagery (aerial monitoring), which yielded the number of pixels representing healthy plant parts and symptomatic plant parts, were analyzed to determine the intensity of the disease. According to McDonald et al. (2022), the measurement of disease intensity in aerial imagery utilizes the following formula[17]:

$$Disease\ Intensity = \frac{\sum lesion\ area(in\ pixel)}{\sum leaf\ area\ (in\ pixel)} \times 100\% \quad (1)$$

In the analysis of distribution patterns, a visual comparison is made between the results of aerial image analysis and the outcomes of geostatistical analysis using ground monitoring observation data [18, 19]. This comparison allows for a comprehensive understanding of the spatial distribution of the disease.

Accuracy was analyzed using a regression correlation statistical test at 95% confidence level using RStudio. The accuracy was calculated by comparing the disease intensity observed in the images with the intensity obtained from the ground monitoring calculations, which served as the actual values [19].

3 Results and Discussion

3.1 Symptoms and Pathogen Identification

Figure 2 displays the symptoms of ring spot disease. These symptoms are characterized by oval to round brownish-white spots with light to dark brown edges. The size of the spots can vary, ranging from shorter to longer than 0.5 cm. This is by Magarey's statement that the size of the spots is 0.1 – 0.5 cm wide and between 0.4 – 1.8 cm long and also has a straw-like (brownish) color, indicating dead tissue on the leaves [2].

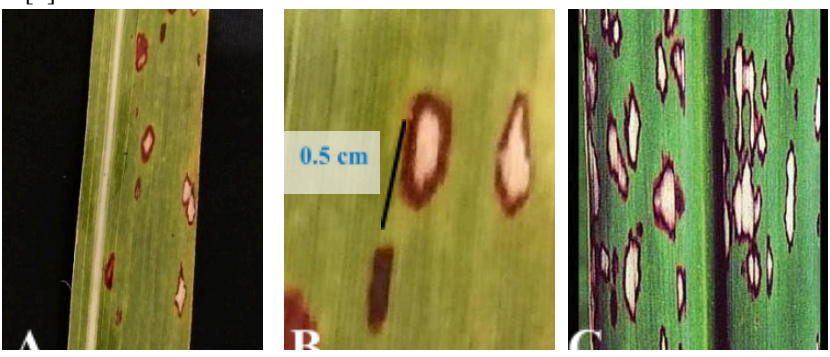

Fig. 2. (A and B) Results of Identification of Symptoms of Ring Spot Disease and (B) Symptoms of Ring Spot Disease according to Magarey [2]

The results of the isolation and in vitro identification confirm that the fungus responsible for ring spot disease is *Leptosphaeria* sp. Taxonomy identification result stated that *Leptosphaeria* sp. is classified within the Ascomycota phylum, Dothideomycetes class, Pleosporales order, and Leptospheriaceae family, as described by Cesati [20]. Figure 3 presents the colonies of Leptosphaeria fungus that were isolated and cultured on Potato Dextrose Agar (PDA) media in Petri dishes. These colonies typically have a diameter ranging from 4 to 6 cm. They exhibit a brownish white to brown color and display a round shape. The texture of the Leptosphaeria colony resembles cotton-like material. In addition, the colony of Leptosphaeria has a texture resembling cotton. Bekele and Kifelw; Nanjundaswamy et al.; and Zarj et al. stated that Leptosphaeria isolated on PDA media formed colonies that were light brown to black [21–23]. It also has a rounded colony shape but tends not to form a perfect circle.

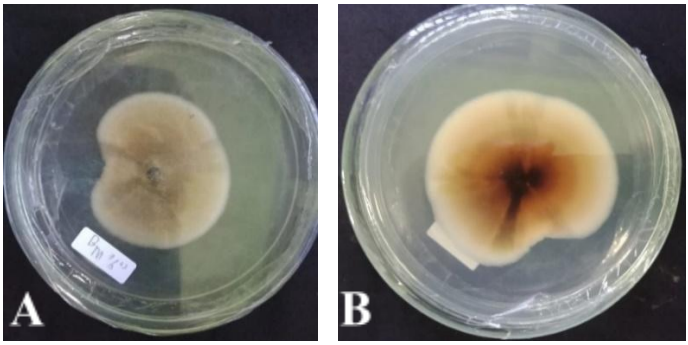

Fig. 3. Colony of *Leptosphaeria* sp. Aged 6 Days After Inoculation on Potato Dextrose Agar (PDA) Media from (A) Top and (B) Bottom Views

Figure 4A presents the results of the identification of *Leptosphaeria* sp. colony using a microscope at 40x magnification. The image displays the hyphae and the asexual reproductive structures of the Leptosphaeria fungus, highlighted within the red circle. Additionally, the image shows the asexual reproductive organs known as conidia, which are one of the characteristic features of the Ascomycota phylum. The hyphae represent the thread-like structures that make up the body of the fungus, and the asexual reproductive structures, such as conidia, are involved in the dispersal and propagation of the fungus. This observation aligns with the classification of *Leptosphaeria* sp. within the Ascomycota phylum, as stated by Cesati [20].

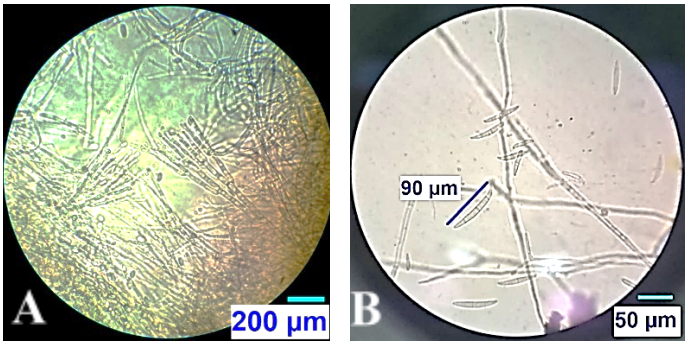

Fig. 4. (A) Hyphae and Conidia of *Leptosphaeria* sp., at 40x Magnification and (B) Conidia of *Leptosphaeria* sp. at 100x Magnification

Figure 4B shows the results of observations at 100x magnification where the conidia of Leptosphaeria are visible. According to the measurement results, it is known that the size of the conidia has a length of 90 µm, has a curved cylindrical shape, has 4 partitions, and tends to be tapered at both ends. Bekele and Kifelw explained that the conidia of Leptosphaeria have a tapered shape at each end [21].

3.2 Aerial Image Acquisition

Image acquisition of sugarcane plantation was conducted on a 1520 m^2 plot with dimensions of 38 m long and 40 m wide. Aerial imagery was collected during the first week and the third week of observation. A total of 28 aerial images were collected with details of 6 columns and 4 rows. The acquired image corresponds to the plot in Figure 5 so that the images do not overlap at one point and another. Image acquisition was carried out at 08.00 UTC+7 at an altitude of 18 m above ground level by following the plot as follows:

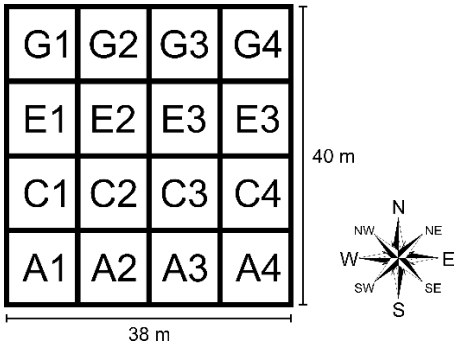

Fig. 5. Aerial Image Acquisition Plan

The images obtained from the observation results have differences in terms of brightness, contrast, and sharpness, resulting in different colors between the first- and

third-week images. Based on the color comparison in Figure 6, the green color in the third week observation results has a brighter color compared to the photo in the first week. The difference in color between the results occurs because it is influenced by the intensity of sunlight received by the plants.

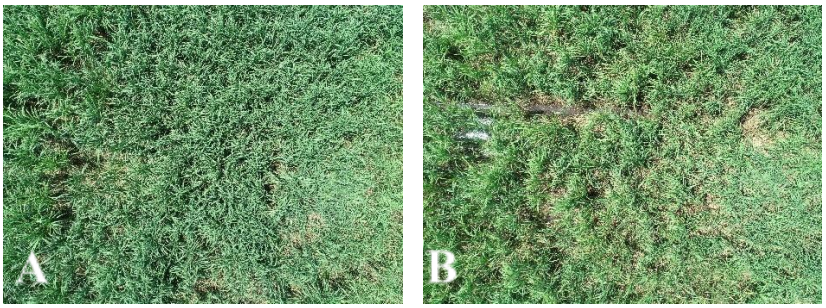

Fig. 6. Aerial Imagery Sample at (A) 1st Week and (B) 3rd Week of Observations

The difference in light intensity received and reflected by plants can result in variations in the electromagnetic (EM) waves at the visual frequency captured by drone cameras [24]. The intensity of light in the field is not always constant when aerial photos are taken [25]. These fluctuations in light intensity can have an impact on the quality of the aerial photos obtained.

These color differences can cause different results during the image segmentation process, which can cause different analysis results. Therefore, a color matching process is carried out on the first week's aerial imagery so that it resembles the third week's aerial image color through the image pre-processing process.

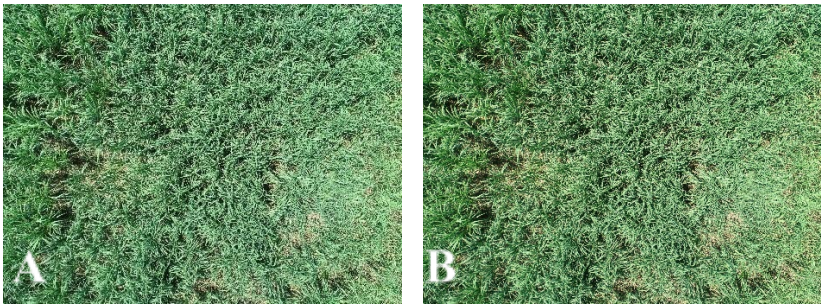

Fig. 7. Aerial Imagery (A) Before Preprocessing (B) After Preprocessing

An aerial image that has not been preprocessed is presented in Figure 7A, an unprocessed image has a characteristic green color that tends to be paler, while Figure 7B shows an image that has a brighter green color. The preprocessing stage involved image enhancement method. Suharyanto and Friyadie stated that image quality can be improved through the image enhancement process, such as color correction through Histogram Equalization [26].

3.3 Aerial Image Processing Results

The first thresholding result (Fig. 8A) was performed to remove the background (soil, dry plant leaves, and irrigation), leaving the sugarcane plant area as a whole. The first thresholding uses three color channels from the *L*a*b* color space. *L*a*b* color space is a color-opponent space with *L** dimension for brightness, *a** and *b** for color dimension. The *L** value ranges from 0 to 100 where 0 indicates black color, while 100 indicates white color. The a* value can have negative and positive values, a negative value in *a** indicates a green color, while a positive *a** value indicates a red color. The *b** value can also be positive and negative, a negative value indicates a blue color, while a positive value is yellow [12].

Fig. 8. Results of (A) First Stage Thresholding, (B) Second Stage Thresholding on Aerial Imagery

The threshold values used in the first stage thresholding process in Figure 8A are as follows: *L*Low = 60; *L*High = 100; *a*Low = -40; *a*High = 20; *b*Low = -20; *b*High = 70. The thresholding results presented by the image in Figure 8A describe the parts of sugarcane plants both healthy and symptomatic to collect the total pixel count of the entire sugarcane plant.

The second stage thresholding is intended to separate the symptomatic plant parts from Figure 8A to produce Figure 8B. The threshold values used are as follows: *L*Low = 84.846; *L*High = 100; *a*Low = -19.574; *a*High = -7.443; *b*Low = -16.905; *b*High = 60. The thresholding results presented by image in Figure 8B explain the part of the sugarcane plant that is symptomatic of ring spot disease with the characteristics of leaves that have brown spots and tend to be yellowish.

The thresholding performed is part of the segmentation while the results of Figure 8A and 8B that have been successfully exported along with the thresholding value are part of the feature extraction. According to Setiawan et al., thresholding is one of the image segmentation methods that separates colors between objects and backgrounds based on certain differences [13].

The results of thresholding in the form of images are calculated to find the intensity of ring spot disease infection through pixel counting operations. Pixel counting produces the number of pixels of symptomatic leaves, healthy leaves, and whole sugarcane plant leaves. The calculation results are then processed to produce plant disease intensity data.

3.4 Aerial Imagery and Geostatistics Analysis

Figure 9. shows that measurements using aerial imagery in the first week have a range of disease intensity ranging from 4% to 13% while the actual intensity in the field ranges from 0 to 25%.

The results of disease detection using aerial imagery, as depicted in Figure 10A, indicate a generally even pattern across the surveyed area. However, there are certain points where disease occurrences tend to cluster or aggregate, suggesting localized concentrations of the disease. On the other hand, the estimation results obtained using kriging based on a spherical variogram, as shown in Figure 10B, reveal a clustered or aggregated distribution of disease at specific points in the Northwest.

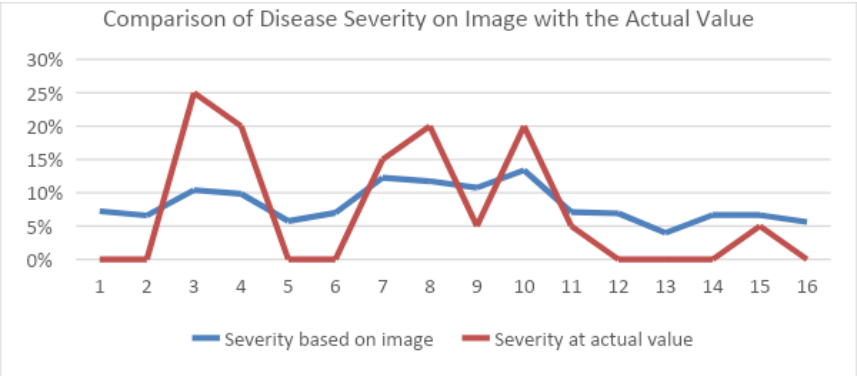

Fig. 9. Comparison of Disease Intensity in the Image with the Actual Value at 1st Week

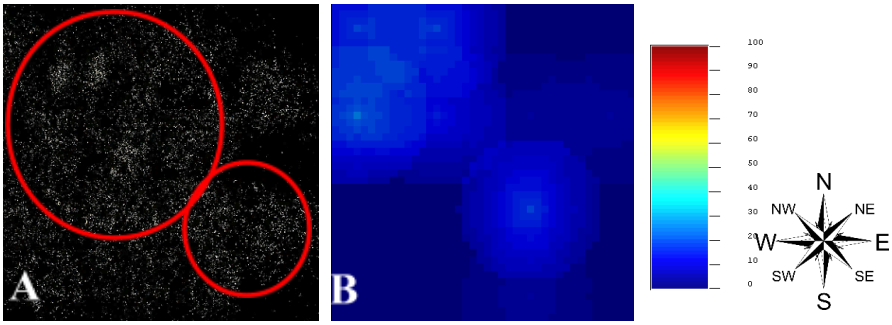

Fig. 10. Disease Distribution Pattern in 1st Week Based on (A) Aerial Imagery (B) Kriging

When compared, the results of disease detection from both methods showed a similarity in terms of the position of disease concentration. This indicates that the areas identified as disease hotspots or clusters in the aerial imagery analysis align with the localized disease concentrations identified through kriging estimation.

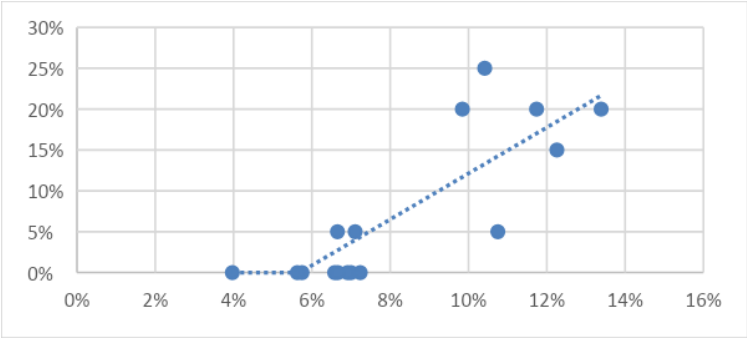

Fig. 11. Comparison of Disease Intensity in Images with the Actual Value of 1st Week Regression Test Results

The patterns observed in both the aerial imagery analysis and kriging estimation exhibit similarities at specific sub-location points. The pattern shown in the figures has a similarity which is validated by the results of the regression correlation test, R2 = 0.69 (Fig. 11). The R determinant value that close to 1 indicates a strong level of correlation. The difference in the results of measuring disease intensity between aerial monitoring and conventional monitoring is influenced by the advantages and disadvantages of each method [19].

Figure 12. shows that measurements using aerial imagery in the third week have a range of disease intensity ranging from 2% to 15% while the actual intensity in the field ranges from 0 to 30%.

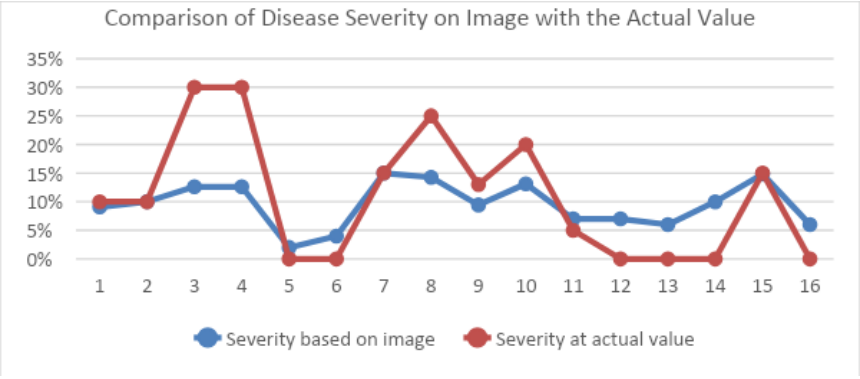

Fig. 12. Comparison of the Disease Intensity in the Image with the Actual Value at 3rd Week

The detection results using aerial imagery (Fig. 13A) show a pattern that tends to aggregate. Meanwhile, the estimation results using kriging based on a spherical variogram (Fig. 13B) show a distribution that is starting to expand from several points in the Northwest to the South and from a point in the center to the South and East. When compared, the detection results from both methods visually show the similarity in the position of disease concentration. This is also corroborated by the statement of

Bande et al. that diseases can be distributed in uniform, random, or in clusters/aggregated [27].

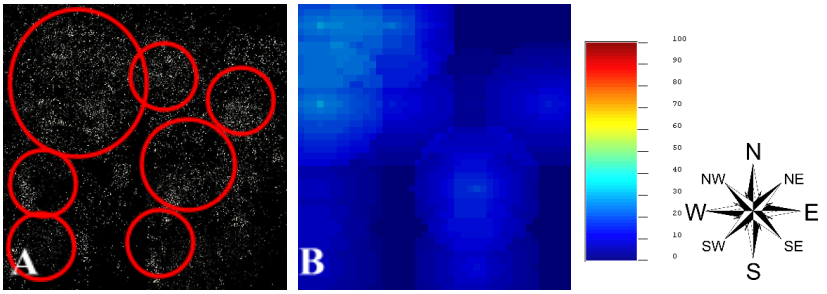

Fig. 13. Disease Distribution Pattern in 3rd Week Based on (A) Aerial Imagery (B) Kriging

The pattern shown in the figure has a similarity which is validated by the results of the regression correlation test, $R^2 = 0.63$ (Fig. 14). The R determinant (R^2) value that close to 1 indicates a strong level of correlation. The difference in the results of measuring disease intensity between aerial monitoring and conventional monitoring is influenced by the advantages and disadvantages of each method [19].

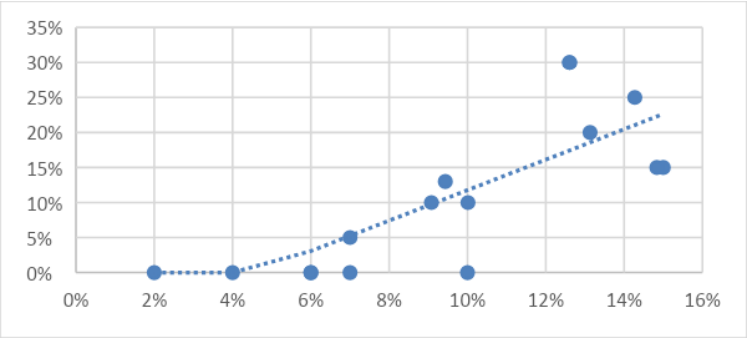

Fig. 14. Comparison of Disease Intensity in Images with the Actual Value at 3rd Week Regression Test Results

According to Lubis et al., conventional observation methods have a disadvantage in that the results are not synoptic, meaning that they may not provide a comprehensive view of the entire area under study [28]. This limitation can lead to potential sampling bias, where the selected observation points may not accurately represent the actual conditions of the entire area. In contrast, observations using aerial imagery offer the advantage of providing synoptic results, allowing for simultaneous observations of the entire area of interest. Furthermore, Kurniantoro et al. stated that aerial imagery allows for measurements at the population level per area [29]. This means that aerial observations can provide data on a larger scale, covering a wider geographic area, and

potentially capturing more representative information about the population being studied. This broader scope enhances the accuracy of the observations obtained through aerial imagery.

4 Conclusion

Aerial imagery acquired using drones has the potential to detect symptoms and distribution patterns of ring spot disease. The accuracy of aerial imagery-based detection is 69±63% based on correlation regression test results. Based on the analysis of aerial imagery and ground monitoring, the distribution of ring spots tends to aggregate. Aerial image-based monitoring from drones or UAVs technically has the advantages of shorter detection time, easier to carry out, and ability to reach areas that are not detected by conventional observation.

5 Suggestion

Based on this research, there are obstacles in detecting symptomatic plant parts that are covered by the canopy, so it is necessary to use a better camera that can take better images and algorithms or programs that improve the accuracy of disease detection.

Acknowledgements. The authors would like to express their gratitude to the Universitas Pembangunan Nasional "Veteran" Jawa Timur for providing the funding support for the publication of this research.

References

1. Jati, W.W., Abadi, A.L., Aini, L.Q., Djauhari, S.: Screening of Trichoderma spp. isolates based on antagonism and chitinolytic index against Xylaria sp. J. Hama dan Penyakit Tumbuh. Trop. 22, 55–67 (2022).
2. Magarey, R.: Diseases of Australian Sugarcane: Field Guide. (2022).
3. Gopi, R., Mahendran, B., Chandran, K., Nisha, M., Viswanathan, R.: Plant and Weather Factors on Resistance of Saccharum officinarum Germplasm Against Ring Spot Disease. Sugar Tech. 23, 720–729 (2021).
4. Indrawan, A.D., Radiyanto, I., Nirwanto, H., Wuryantini, S.: Geospatial Study On The Existence Of Citrus Pest Myllocerus sp. (Coleoptera: Curculionidae) In Dau Subdistrict, Malang District. In: 1st International Conference on Agriculture Proceeding. pp. 210–218 (2020).
5. Nirwanto, H., Lestari, M.P.: Spatial Distribution Patterns of Fungal Disease in Shallot Crop. In: 1st International Conference on Agriculture Proceeding. pp. 236–243 (2020).
6. Hafeez, A., Husain, M.A., Singh, S.P., Chauhan, A., Khan, M.T., Kumar, N., Chauhan, A., Soni, S.K.: Implementation of drone technology for farm monitoring & pesticide spraying: A review. Inf. Process. Agric. 10, 192–203 (2023).
7. Abbas, A., Zhang, Z., Zheng, H., Murtaza Alami, M., Alrefaei, A.F., Abbas, Q., Atif Hasan Naqvi, S., Junaid Rao, M., A Mosa, W.F., Hussain, A., Zeeshan Hassan, M., Zhou, L.: Drones in Plant Disease Assessment, Efficient Monitoring, and Detection: A Way Forward to Smart Agriculture. (2023).

8. Haikal, M.R., Nirwanto, H., Mujoko, T.: Kajian Pola Sebaran Penyakit Bulai Dengan Analisis Citra Drone. J. AGROHITA J. Agroteknologi Fak. Pertan. Univ. Muhammadiyah Tapanuli Selatan. 7, 242–248 (2022).
9. Akram, T., Naqvi, S.R., Haider, S.A., Kamran, M.: Towards real-time crops surveillance for disease classification: exploiting parallelism in computer vision. Comput. Electr. Eng. 59, 15–26 (2017).
10. Abdullah, S.K., Salih, Y.A.: Mycobiota associated with sugarcane (Saccharum officinarum L.) in Iraq. J. Biol. Sci. 3, 193–202 (2010).
11. Prabowo, D.A., Abdullah, D., Manik, A.: Deteksi dan Perhitungan Objek Berdasarkan Warna Menggunakan Color Object Tracking. Pseudocode. 5, 85–91 (2018).
12. Mentari, M., Ginardi, H., Fatichah, C.: Segmentasi Penyakit Pada Citra Daun Tebu Menggunakan Fuzzy C Means – Support Vector Machine Dengan Fitur Warna a*. JUTI J. Ilm. Teknol. Inf. 13, 45 (2015).
13. Setiawan, I., Dewanta, W., Nugroho, H.A., Supriyono, H., Tetap Program, D., Manajemen, S., Amik, I., Surakarta, H.B., Yani, J.A., Kartasura, K., Sukoharjo, K.: Pengolah Citra Dengan Metode Thresholding Dengan Matlab R2014A. J. MEDIA INFOTAMA. 15, 639763 (2019).
14. Thenmozhi, K., Reddy, U.S.: Image processing techniques for insect shape detection in field crops. Proc. Int. Conf. Inven. Comput. Informatics, ICICI 2017. 699–704 (2018).
15. Remy, N., Boucher, A., Wu, J.: Applied Geostatistics with SGeMS: A user's guide. Appl. Geostatistics with SGeMS A User's Guid. 9780521514149, 1–264 (2009).
16. Belan, L.L., Pozza, E.A., Alves, M. de C., Freitas, M.L. de O.: Geostatistical analysis of bacterial blight in coffee tree seedlings in the nursery. Summa Phytopathol. 44, 317–325 (2018).
17. McDonald, S.C., Buck, J., Li, Z.: Automated, image-based disease measurement for phenotyping resistance to soybean frogeye leaf spot. Plant Methods. 18, 1–11 (2022).
18. Amara, K., Nirwanto, H., Harijani, W.S., Imanadi, L.: Model Perkembangan Penyakit Bulai pada Berbagai Varietas di Kabupaten Mojokerto. Plumula Berk. Ilm. Agroteknologi. 8, 9–22 (2020).
19. Setiawan, J., Nirwanto, H., Windriyanti, W.: Estimation of Yield Damage Due to Whitefly Pest Attack on Cayenne Pepper Plants Based on Drone Imagery| Himalayan Journals. Himal. J. Agric. 4, 1–6 (2023).
20. Cesati, V.: Schema di classificazione degle sferiacei italici aschigeri piu' o meno appartenenti al genere Sphaeria nell'antico significato attribuitoglide Persono. (1863).
21. Bekele, B., Kifelw, H.: Distribution, Virulence and Diversity of Leptosphaeria maculans and Leptoshaeria biglobusa at Major Brassica Growing Areas of Ethiopia. J. Plant Pathol. Microbiol. 11, 1–6 (2020).
22. Nanjundaswamy, J., Naik, S., Nandan, M.: Efficacy of fungicides, biocontrol agents and botanicals against ring spot disease (Leptosphaeria sacchari Van de Brenda) of sugarcane. J. Pharmacogn. Phytochem. 9, 304–307 (2020).
23. Vakili zarj, Z., Rahnama, K., Nasrollanejad, S., Yamchi, A.: Morphological and molecular identification of Leptosphaeria maculans in canola seeds and flowers collected from the North Iran. Arch. Phytopathol. Plant Prot. 50, 526–539 (2017).
24. Sulistiyanti, S.R., Setyawan, F.X.A., Komarudin, M.: Pengolahan Citra Dasar dan Contoh Penerapannya. (2016).
25. Putra, H., Prasetyo, L.B., Santoso, N.: Monitoring Perubahan Garis Pantai dengan Citra Satelit di Gembong Bekasi. J. Pengelolaan Sumberd. Alam dan Lingkung. (Journal Nat. Resour. Environ. Manag. 6, 178 (2016).
26. Suharyanto, S., Frieyadie, F.: Analisis Komparasi Perbaikan Kualitas Citra Bawah Air Berbasis Kontras Pemerataan Histogram. INTI Nusa Mandiri. 15, 95–102 (2020).
27. Bande, L.O.S., Hadisutrisno, B., Somowiyarjo, S.: Pola Agihan dan Intensitas Penyakit Busuk Pangkal Batang Lada di Provinsi Sulawesi Tenggara. J. Agroteknos. 4, (2014).

28. Lubis, M.Z., Gustin, O., Anurogo, W., Kausarian, H., Anggraini, K., Hanafi, A.: Penerapan Teknologi Pengideraan Jauh Di Bidang Pesisir Dan Lautan. OSEANA. 42, 56–64 (2017).
29. Kurniantoro, A., Hermantoro, A., Ika, U., Jurusan, T., Pertanian, T., Pertanian, I., Pertanian, S., Yogyakarta, J.: Pemanfaatan Drone Terintegrasi SIG untuk Pemetaan Tanaman Jagung. Agric. Eng. Innov. J. 1, 47–60 (2023).